

A synchrotron X-ray study of triclinic $\text{LiCa}_2\text{Nb}_3\text{O}_{10}$ with perovskite-type slabs

Nobuo Ishizawa,^{a*} Reiko Yamashita,^a Shuji Oishi,^b
James R. Hester^c and Shunji Kishimoto^d

^aMaterials and Structures Laboratory, Tokyo Institute of Technology, Nagatsuta, Midori, Yokohama 226-8503, Japan, ^bDepartment of Environmental Science and Technology, Faculty of Engineering, Shinshu University, Wakasato, Nagano 380-8553, Japan, ^cAustralian Nuclear Science and Technology Organisation, PMB 1, Menai, NSW 2234, Australia, and ^dInstitute of Materials Structure Science, High Energy Accelerator Research Organization, 1-1 Oho, Tsukuba 305-0801, Japan
Correspondence e-mail: nishizaw@n.cc.titech.ac.jp

Received 11 May 2001

Accepted 6 June 2001

The triclinic superstructure of a small crystal of $\text{LiCa}_2\text{Nb}_3\text{O}_{10}$, lithium dicalcium triniobium decaoxide, has been investigated by synchrotron X-ray diffraction. The unit cell is an almost rectangular parallelepiped, although there is a 0.245° offset from orthogonality for β . The structure essentially belongs to a homologous series of $\text{Li}[\text{Na}_{n-3}\text{Ca}_2\text{Nb}_n\text{O}_{3n+1}]$ with $n = 3$, where the moiety in square brackets has a perovskite-type slab structure. The superstructure has a doubled unit-cell volume with respect to the tetragonal aristotype. The NbO_6 octahedra are rotated about axes parallel to $[110]$ by approximately 10° . Adjacent slabs are connected by Li atoms and are geometrically related by 4_2 pseudosymmetry lying parallel to \mathbf{c} . There are twice as many sites as Li atoms, providing a variation of population at these Li sites.

Comment

Recently, layered perovskite-type compounds, $A\text{Ca}_2\text{Nb}_3\text{O}_{10}$, with $A = \text{Li, Na, K, Rb}$ or Cs , have attracted attention because they possess properties such as superconductivity (Fukuoka *et al.*, 1997; Takano *et al.*, 1997), luminescence (Bizeto *et al.*, 2000) and photocatalytic behaviour for overall water splitting (Takata *et al.*, 1998). These layered perovskites belong to a homologous series of general formula $A[\text{Na}_{n-3}\text{Ca}_2\text{Nb}_n\text{O}_{3n+1}]$, with $n = 3$. In this notation, the moiety in square brackets denotes the perovskite-type slab, with n corresponding to the number of NbO_6 octahedra across the slab. The A atom outside the brackets is located at the interlayer and joins adjacent slabs.

Although the aristotype structure of $A\text{Ca}_2\text{Nb}_3\text{O}_{10}$ has tetragonal symmetry, detailed analyses based on single-crystal X-ray diffraction suggest lower symmetries. For example, $\text{CsCa}_2\text{Nb}_3\text{O}_{10}$ is orthorhombic, space group $Pnam$ (Dion *et al.*, 1984), and $\text{KCa}_2\text{Nb}_3\text{O}_{10}$ is orthorhombic, space group $Cmcm$

(Fukuoka *et al.*, 2000). A single-crystal structure analysis of $\text{LiCa}_2\text{Nb}_3\text{O}_{10}$, (I), has not been undertaken prior to this work, mainly due to the small size of the crystals, the presence of twinning and poor crystallinity. However, in the present study, several crystals grown in Li_2SO_4 flux were found to be tolerable for single-crystal diffraction using synchrotron radiation. The triclinic structure of $\text{LiCa}_2\text{Nb}_3\text{O}_{10}$ has thus been determined at the Photon Factory, High Energy Accelerator Research Organization, Tsukuba, and the results are presented here.

In the structure of (I), there are two crystallographically independent slabs, composed of Nb, Ca and O atoms, and labelled with even and odd numbers, respectively. These slabs are stacked alternately along \mathbf{c} , as shown in Figs. 1 and 2. The Ca atom has 12-fold coordination. The corner-linked NbO_6 octahedra are rotated relative to each other by approximately 10° . The dominant component of the rotation occurs about axes parallel to $[110]$. There is also a trace rotation component about $[001]$ for the Nb1O_6 , Nb2O_6 , Nb5O_6 and Nb6O_6 octahedra. The dominant rotation axes align parallel within a slab, while they are flipped by 90° in adjacent slabs, as shown in Fig. 2. As a result, the slabs are geometrically related by 4_2 pseudosymmetry along \mathbf{c} , if the 0.245° offset from orthogonality is neglected for β . This $P\bar{1}$ structure, in which two similar layers are rotated relative to each other by 90° around their normal, is also found in $\text{K}_2\text{Cr}_2\text{O}_7$ (Brandon & Brown, 1968).

Displacement of the Nb atom from the centre of the coordination octahedron along \mathbf{c} is notable for Nb3, Nb4, Nb7 and Nb8 on the outer side of the slab, while none is observed for

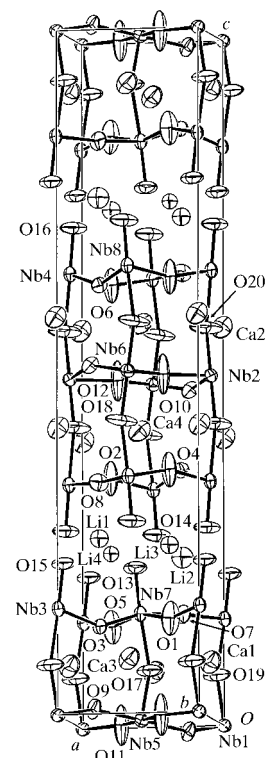


Figure 1

The structure of (I) with displacement ellipsoids at the 90% probability level.

Nb1, Nb2, Nb5 and Nb6 at the inversion centres. The electric dipoles induced by off-centre displacements of the former group of Nb atoms cancel each other within each slab.

Adjacent slabs are joined together by Li atoms located at the interlayer, as shown in Fig. 3. They have essentially tetrahedral coordination, although the rotation of NbO_6 octahedra appends to Li1 and Li2 another Li—O bond, which is shorter than two of the tetrahedral ones. These extra Li—O bonds exist along directions nearly parallel to **c**. The O atoms surrounding the Li atom tetrahedrally occupy diagonal corners of a pseudo-cube, with dimensions of approximately 2.74 Å along **a** and **b**, and 1.53 Å along **c**. These cubes are significantly compressed along **c**, by 1.21 Å. This is partly due to the rotation of the NbO_6 octahedra in the perovskite-type slab.

There are twice as many sites as Li atoms, providing a variation of population at these Li sites. The fivefold Li1 and Li2 sites have populations approximately twice as large as the fourfold Li3 and Li4 sites. The excess number of Li sites may enable Li diffusion along the interlayers in the crystal. From symmetry constraints, there is only one crystallographically independent interlayer structure composed of Li atoms in the unit cell.

Depending on which Li sites are occupied, the O atoms near the interlayer could be displaced one way or the other from their refined average positions. This would result in local changes of the rotation angles of the NbO_6 octahedra, an effect that would be transmitted across the slab or at least to the octahedron in the centre of the slab. The large anisotropy of the atomic displacement parameters of several O atoms

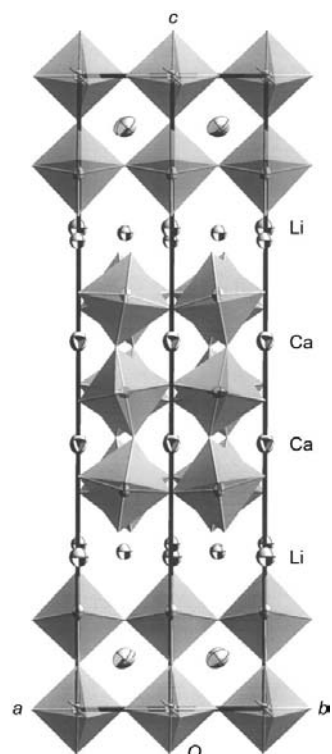


Figure 2
A polyhedral view of (I) along [110]. Displacement ellipsoids of Li and Ca atoms are drawn at the 90% probability level.

therefore probably represents static disorder rather than thermal motion. The 2:1 ratio in the occupancies of the Li sites is suggestive of a possible long-range modulation with a tripled *c*-axis periodicity. However, the present X-ray study using both area and counter detectors revealed no such modulation along **c**. It is possible that a longer annealing time would allow such a modulation to develop in the present crystal.

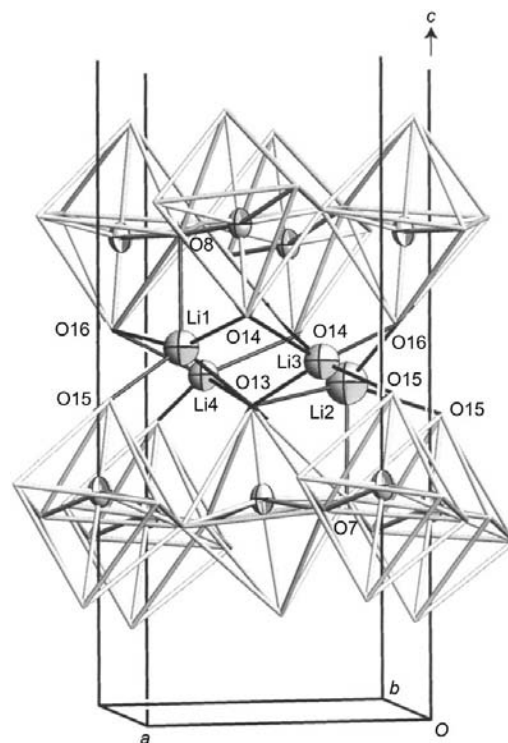


Figure 3
The interlayer moiety near the plane at $z = \frac{1}{4}$. Displacement ellipsoids of Li and Nb atoms are drawn at the 90% probability level.

Dion *et al.* (1981) reported a tetragonal unit cell of $a = 7.720$ (7) and $c = 28.331$ (3) Å for (I). If a tetragonal aristotype with unit-cell vectors of \mathbf{a}_0 , \mathbf{b}_0 and \mathbf{c}_0 is considered, the structure of Dion *et al.* (1981) can be expressed as $\mathbf{a} \simeq 2\mathbf{a}_0$, $\mathbf{b} \simeq 2\mathbf{b}_0$ and $\mathbf{c} \simeq \mathbf{c}_0$, and the present structure as $\mathbf{a} \simeq \mathbf{a}_0 + \mathbf{b}_0$, $\mathbf{b} \simeq \mathbf{a}_0 - \mathbf{b}_0$ and $\mathbf{c} \simeq \mathbf{c}_0$. The unit-cell volume of the present structure is twice as large as the aristotype and half as large as that of Dion *et al.* (1981). No superstructure reflections indicative of the latter structure were observed in the present study.

It is notable that the *c* length of the present crystal is approximately 7% (1.778 Å) shorter than that reported for the crystal of Dion *et al.* (1981). This suggests the possible existence of two phases with the same or slightly different compositions. A similar phenomenon was also observed for flux-grown $\text{Na}[\text{NaCa}_2\text{Nb}_4\text{O}_{13}]$ crystals belonging to the homologous series with $n = 4$ (Chiba *et al.*, 1999).

The present crystal of (I) has triclinic $P\bar{1}$ symmetry with monoclinic cell dimensions. Such apparent symmetry enhancement is also found in another layered perovskite-type compound, $\text{Bi}_4\text{Ti}_3\text{O}_{12}$, which has a monoclinic symmetry with orthorhombic cell dimensions (Rae *et al.*, 1990).

Experimental

Single crystals of (I) were grown by the flux method using Li_2SO_4 as flux. Reagent grade CaCO_3 , Nb_2O_5 and Li_2SO_4 were weighed and mixed together to form a nominal composition of 1 mol% $\text{LiCa}_2\text{Nb}_3\text{O}_{10}$. A platinum crucible containing a mixture of approximately 5 g was heated to 1373 K at the rate of 45 K h^{-1} in an air atmosphere, kept at 1373 K for 2 h, cooled to 723 K at 5 K h^{-1} and then discharged. The flux was rinsed out with water at 353 K. Thin crystals with a maximum size of $0.2 \times 0.2 \times 0.1 \text{ mm}$ were identified as $\text{LiCa}_2\text{Nb}_3\text{O}_{10}$ by chemical analysis using an energy dispersive X-ray spectrometer and X-ray diffraction. An additional product with hexagonal faces was identified as Li_3NbO_4 .

Crystal data

$\text{LiCa}_2\text{Nb}_3\text{O}_{10}$	$D_x = 4.379 \text{ Mg m}^{-3}$
$M_r = 525.83$	Synchrotron radiation
Triclinic, $P\bar{1}$	$\lambda = 0.75008 (2) \text{ \AA}$
$a = 5.4809 (3) \text{ \AA}$	Cell parameters from 24 reflections
$b = 5.4804 (3) \text{ \AA}$	$\theta = 32.5\text{--}50.7^\circ$
$c = 26.5533 (16) \text{ \AA}$	$\mu = 5.57 \text{ mm}^{-1}$
$\alpha = 89.999 (4)^\circ$	$T = 293 (2) \text{ K}$
$\beta = 90.245 (4)^\circ$	Irregular, colourless
$\gamma = 89.999 (5)^\circ$	$0.06 \times 0.05 \times 0.03 \text{ mm}$
$V = 797.59 (8) \text{ \AA}^3$	
$Z = 4$	

Data collection

KEK BL14A four-circle diffractometer	$R_{\text{int}} = 0.021$
$\omega/2\theta$ scans	$\theta_{\text{max}} = 32.5^\circ$
Absorption correction: analytical (de Meulenaer & Tompa, 1965)	$h = -7 \rightarrow 7$
$T_{\text{min}} = 0.598$, $T_{\text{max}} = 0.885$	$k = 0 \rightarrow 7$
5607 measured reflections	$l = -38 \rightarrow 38$
4904 independent reflections	8 standard reflections
3750 reflections with $I > 2\sigma(I)$	every 200 reflections
	intensity decay: none

Refinement

Refinement on F^2	$w = 1/[\sigma^2(F_o^2) + (0.101P)^2 + 5.14P]$
$R(F) = 0.051$	where $P = (F_o^2 + 2F_c^2)/3$
$wR(F^2) = 0.169$	$(\Delta/\sigma)_{\text{max}} = 0.002$
$S = 0.94$	$\Delta\rho_{\text{max}} = 2.13 \text{ e \AA}^{-3}$
4904 reflections	$\Delta\rho_{\text{min}} = -4.03 \text{ e \AA}^{-3}$
297 parameters	

A preliminary examination of the crystals was carried out using an Imaging Plate diffractometer (Rigaku RAPID). A crystal of approximately $60 \times 46 \times 25 \mu\text{m}$ along the $[110]$, $[\bar{1}10]$ and $[001]$ directions, respectively, was chosen from a number of crystal fragments. No clear indication of twinning was observed for the crystal. Monoclinic distortion was suggested from the preliminary examination and confirmed by further study using synchrotron radiation. Diffraction data were obtained using a horizontal-type four-circle diffractometer at beamline 14 A of the Photon Factory (Satow & Iitaka, 1989). Vertically polarized X-rays of $\lambda = 0.75008 (2) \text{ \AA}$ were obtained using an Si double-crystal monochromator. The wavelength was calibrated using a spherically ground Si standard crystal. Although most reflections were quite weak at high angles of about $2\theta > 65^\circ$, several parent structure reflections and their equivalents still had sharp profiles in the region. Cell dimensions were thus determined using 24 of those reflections. An eight-channel avalanche photodiode detector was used for photon counting (Kishimoto *et al.*, 1998). The aperture of the detector was approximately 6 mrad. The detection efficiency was approximately 75% at this wavelength. Since the dynamic range of the detector exceeds 10^8 c.p.s., no attenuator or absorber was used for data collection. The maximum recorded count

Table 1

Selected bond lengths (\AA).

Nb1—O19 ($\times 2$)	1.934 (3)	Ca2—O4 ^{xi}	2.446 (3)
Nb1—O11 ⁱ ($\times 2$)	1.985 (3)	Ca2—O2 ^{xii}	2.505 (4)
Nb1—O9 ⁱⁱ ($\times 2$)	2.011 (3)	Ca2—O6 ⁱ	2.506 (4)
Nb2—O20 ($\times 2$)	1.933 (3)	Ca2—O8 ^{vii}	2.753 (3)
Nb2—O12 ⁱ ($\times 2$)	1.981 (3)	Ca2—O10	2.926 (3)
Nb2—O10 ($\times 2$)	2.008 (3)	Ca2—O18 ^{xiii}	3.083 (5)
Nb3—O15	1.792 (3)	Ca2—O20 ^{viii}	3.083 (4)
Nb3—O1 ⁱⁱⁱ	1.962 (4)	Ca2—O12 ⁱ	3.188 (4)
Nb3—O7 ^{iv}	1.971 (3)	Ca2—O12 ^{xii}	3.192 (4)
Nb3—O5 ^v	1.982 (4)	Ca3—O3 ^{viii}	2.392 (3)
Nb3—O3	1.996 (3)	Ca3—O19	2.500 (5)
Nb3—O19 ^{iv}	2.235 (4)	Ca3—O17	2.506 (4)
Nb4—O16	1.791 (3)	Ca3—O5	2.557 (4)
Nb4—O2 ^{vi}	1.956 (3)	Ca3—O1 ^{viii}	2.565 (4)
Nb4—O8 ^{vi}	1.974 (3)	Ca3—O11	2.578 (5)
Nb4—O6	1.977 (3)	Ca3—O11 ^{xiv}	2.582 (5)
Nb4—O4 ^{vii}	1.996 (3)	Ca3—O7	2.834 (3)
Nb4—O20 ⁱⁱⁱ	2.235 (4)	Ca3—O9 ^{viii}	2.933 (3)
Nb5—O17 ($\times 2$)	1.935 (3)	Ca3—O17 ^{viii}	3.014 (4)
Nb5—O11 ($\times 2$)	1.983 (3)	Ca3—O19 ⁱⁱⁱ	3.020 (5)
Nb5—O9 ($\times 2$)	2.008 (3)	Ca3—O9 ^x	3.347 (3)
Nb6—O18 ^{viii} ($\times 2$)	1.935 (3)	Ca4—O4 ^{vii}	2.394 (3)
Nb6—O12 ($\times 2$)	1.985 (3)	Ca4—O20	2.506 (5)
Nb6—O10 ($\times 2$)	2.010 (3)	Ca4—O18 ^{vii}	2.508 (4)
Nb7—O13	1.791 (3)	Ca4—O6	2.560 (4)
Nb7—O5	1.957 (4)	Ca4—O2 ^{vii}	2.562 (4)
Nb7—O7	1.975 (3)	Ca4—O12	2.581 (5)
Nb7—O1	1.976 (4)	Ca4—O12 ^{vii}	2.586 (5)
Nb7—O3	1.994 (3)	Ca4—O8 ^{vii}	2.837 (3)
Nb7—O17	2.233 (4)	Ca4—O10 ^{vii}	2.940 (3)
Nb8—O14 ^{vii}	1.796 (3)	Ca4—O18 ^{ix}	3.010 (4)
Nb8—O6 ^v	1.961 (3)	Ca4—O20 ⁱⁱⁱ	3.013 (5)
Nb8—O8 ^{ix}	1.973 (3)	Ca4—O10	3.346 (3)
Nb8—O2 ^{vii}	1.981 (3)	Li1—O15	1.962 (12)
Nb8—O4 ^{vii}	1.993 (3)	Li1—O13	1.975 (12)
Nb8—O18 ^{ix}	2.231 (4)	Li1—O8	2.180 (14)
Ca1—O9 ⁱ	2.392 (3)	Li1—O14 ^v	2.224 (12)
Ca1—O17	2.430 (5)	Li1—O16 ^{vi}	2.289 (12)
Ca1—O19	2.434 (4)	Li2—O16 ^{vii}	1.937 (12)
Ca1—O3 ⁱ	2.444 (3)	Li2—O14	1.981 (12)
Ca1—O1	2.499 (4)	Li2—O7	2.205 (14)
Ca1—O5 ⁱ	2.505 (4)	Li2—O13	2.262 (12)
Ca1—O7	2.754 (3)	Li2—O15 ⁱⁱ	2.274 (12)
Ca1—O9 ^x	2.933 (3)	Li3—O13	2.07 (2)
Ca1—O19 ^v	3.084 (4)	Li3—O16 ^{vii}	2.11 (2)
Ca1—O17 ⁱ	3.087 (5)	Li3—O15 ⁱ	2.11 (2)
Ca1—O11 ⁱ	3.193 (4)	Li3—O14 ^v	2.12 (2)
Ca1—O11 ^x	3.196 (4)	Li4—O15 ^{viii}	2.06 (2)
Ca2—O10 ^{xi}	2.393 (3)	Li4—O16 ^{vi}	2.10 (2)
Ca2—O18 ^{vii}	2.434 (5)	Li4—O14	2.12 (2)
Ca2—O20	2.434 (4)	Li4—O13	2.12 (2)

Symmetry codes: (i) $x - 1, y, z$; (ii) $x - 1, y - 1, z$; (iii) $1 + x, y, z$; (iv) $1 + x, 1 + y, z$; (v) $x, 1 + y, z$; (vi) $2 - x, 1 - y, 1 - z$; (vii) $1 - x, 1 - y, 1 - z$; (viii) $x, y - 1, z$; (ix) $1 - x, 2 - y, 1 - z$; (x) $1 - x, 1 - y, -z$; (xi) $-x, -y, 1 - z$; (xii) $1 - x, -y, 1 - z$; (xiii) $-x, 1 - y, 1 - z$; (xiv) $1 - x, -y, -z$.

rate for the present crystal was approximately 1.4×10^6 c.p.s., for the 020 reflection. The half-width at half maximum was approximately 0.13° in ω for strong reflections at low angles. Absorption coefficients were taken from Sasaki (1990). The unit cell has a monoclinic shape. As listed in the *Crystal Data*, the determination of cell dimensions assuming a triclinic cell revealed a significant though small offset for β , but no significant offsets from orthogonality for α and γ . The intensity statistics of the parity groups of the measured reflections suggested that there were no systematic absences for hkl except for $0k0$ with k odd. Accordingly, the possibility of glide planes or centred lattices was discarded. For example, the existence of five reflections with $I > 3\sigma(I)$ for $h0l$ with h odd eliminated the a -glide plane perpendicular to \mathbf{b} in the monoclinic cell with the b axis unique. Therefore, the crystal was assumed to have monoclinic $P12_1$

symmetry until the final stage of refinement. After the structure was solved with $P12_11$, the possible existence of extra pseudosymmetries, for example, a fourfold axis along **c** and mirror planes perpendicular to **a** or **b**, was suggested by the programs *BUNYIP* (Hester & Hall, 1996) and *PLATON* (Spek, 2001). Most of these extra symmetries are the remains of the tetragonal aristotype with $I4/mmm$ symmetry, and are incompatible with the rotation scheme of corner-linked NbO_6 octahedra in the perovskite-type slab. These symmetries disappeared when the match tolerance was reduced to 0.2 Å in *BUNYIP*. However, it was difficult to eliminate the possibility of inversion centres completely, because only the Li and several O-atom positions were displaced more than three s.u.'s from the theoretical centrosymmetric positions. Since the monoclinic space groups containing mirrors can be excluded by the geometrical problems they would cause for octahedral rotation, there are no monoclinic centrosymmetric space groups in accord with the observed extinction rules for reflections. Therefore, triclinic $P\bar{1}$ symmetry was tested finally and the results were compared with those of $P12_11$. The R factor assuming $P12_11$ was 0.062 for 187 parameters and 2037 independent reflections, employing anisotropic atomic displacement parameters (ADPs) for Nb and Ca, and isotropic ADPs for O and Li atoms. The corresponding R factor assuming $P\bar{1}$ was 0.073 for 194 parameters and 3750 independent reflections. A trial to refine the Li population parameters jointly with the other parameters was unsuccessful in the $P12_11$ model. Therefore, the Li populations were fixed at values which gave moderate isotropic ADPs. No such problems occurred in the $P\bar{1}$ model. The $P12_11$ refinement gave an R factor of 0.042 for 291 parameters using anisotropic ADPs for Nb, Ca and O atoms, and isotropic ADPs for Li. Although the R factor was smaller than that obtained for $P\bar{1}$ as given in the *Crystal Data*, it was difficult to ascertain the plausibility of the $P12_11$ model because of the following reservations: first, the apparent superiority of the R factor is considerably reduced when one considers that the number of reflections used is almost halved for $P12_11$ while the number of parameters is approximately the same; secondly, the anisotropic ADPs of several O atoms converged at non-positive definite values; and thirdly, the population parameters of Li did not converge when refined together with the Li isotropic ADPs. On the other hand, the $P\bar{1}$ refinement converged smoothly, employing anisotropic ADPs for Nb, Ca and O atoms, and isotropic ADPs for Li, refined together with the population parameters of Li. Although the ADP of atom O12 is a prolate spheroid with a max/min ratio of 4.2, the ADPs for all O atoms were much improved compared with the results obtained for the $P12_11$ model. Thus, space group $P\bar{1}$ was adopted for the present crystal. The major reason for the removal of the twofold screw symmetries lies in the interlayer structure, *i.e.* the positional shifts of Li atoms and their distribution among the available sites. In the final difference Fourier maps, a negative difference electron density of $-4.03 \text{ e } \text{Å}^{-3}$ was found 0.24 Å from Ca2.

Data collection: *DIFF14A* (Vaalsta & Hester, 1997); cell refinement: *Xtal3.4* (Hall *et al.*, 1995); data reduction: *Xtal3.4*; program(s) used to solve structure: *SHELXS97* (Sheldrick, 1997); program(s) used to refine structure: *SHELXL97* (Sheldrick, 1997); molecular graphics: *ORTEP* (Johnson, 1970) and *ATOMS* (Dowty, 1995).

The study was supported by Grants-in-Aid for Scientific Research on Priority Areas (B) No. 740, and also Nos. 11450245 and 12875120, from the Ministry of Education, Culture, Sports, Science and Technology, Japan. The synchrotron experiments at the Photon Factory were performed based on program 99G190.

Supplementary data for this paper are available from the IUCr electronic archives (Reference: BR1337). Services for accessing these data are described at the back of the journal.

References

- Bizeto, M. A., Constantino, V. R. L. & Brito, H. F. (2000). *J. Alloys Compd.* **311**, 159–168.
- Brandon, J. K. & Brown, I. D. (1968). *Can. J. Chem.* **46**, 933–941.
- Chiba, K., Ishizawa, N. & Oishi, S. (1999). *Acta Cryst.* **C55**, 1041–1044.
- Dion, M., Ganne, M. & Tournoux, M. (1981). *Mater. Res. Bull.* **16**, 1429–1435.
- Dion, M., Ganne, M., Tournoux, M. & Ravez, J. (1984). *Rev. Chim. Miner.* **21**, 92–103.
- Dowty, E. (1995). *ATOMS*. Version 5.1b. Shape Software, 521 Hidden Valley Road, Kingsport, TN 37663, USA.
- Fukuoka, H., Isami, T. & Yamanaka, S. (1997). *Chem. Lett.* pp. 703–704.
- Fukuoka, H., Isami, T. & Yamanaka, S. (2000). *J. Solid State Chem.* **151**, 40–45.
- Hall, S. R., King, G. S. D. & Stewart, J. M. (1995). Editors. *Xtal3.4 User's Manual*. University of Western Australia, Perth: Lamb.
- Hester, J. R. & Hall, S. R. (1996). *J. Appl. Cryst.* **29**, 474–478.
- Johnson, C. K. (1970). *ORTEP*. Report ORNL-3794, 2nd revision. Oak Ridge National Laboratory, Tennessee, USA.
- Kishimoto, S., Ishizawa, N. & Vaalsta, T. P. (1998). *Rev. Sci. Instrum.* **69**, 384–391.
- Meulenaer, J. de & Tompa, H. (1965). *Acta Cryst.* **19**, 1014–1018.
- Rae, A. D., Thompson, J. G., Withers, R. L. & Willis, A. C. (1990). *Acta Cryst.* **B46**, 474–487.
- Sasaki, S. (1990). KEK Report 90-16, pp. 7–26. National Laboratory for High Energy Physics, Tsukuba, Japan.
- Satow, Y. & Iitaka, Y. (1989). *Rev. Sci. Instrum.* **60**, 2390–2393.
- Sheldrick, G. M. (1997). *SHELXL97* and *SHELXS97*. University of Göttingen, Germany.
- Spek, A. L. (2001). *PLATON*. University of Utrecht, The Netherlands.
- Takano, Y., Takayanagi, S., Ogawa, S., Yamadaya, T. & Mori, N. (1997). *Solid State Commun.* **103**, 215–217.
- Takata, T., Tanaka, A., Hara, M., Kondo, J. & Domen, K. (1998). *Catal. Today*, **44**, 17–26.
- Vaalsta, T. P. & Hester, J. R. (1997). *DIFF14A*. Photon Factory, Tsukuba, Japan.